



## Factors Affecting Site-Specific Response Analysis

G. Tönük & A. Ansal

To cite this article: G. Tönük & A. Ansal (2022): Factors Affecting Site-Specific Response Analysis, Journal of Earthquake Engineering, DOI: [10.1080/13632469.2021.1991518](https://doi.org/10.1080/13632469.2021.1991518)

To link to this article: <https://doi.org/10.1080/13632469.2021.1991518>



Published online: 18 Jan 2022.



Submit your article to this journal [↗](#)



Article views: 38



View related articles [↗](#)



View Crossmark data [↗](#)



# Factors Affecting Site-Specific Response Analysis

G. Tönük<sup>a</sup> and A. Ansal <sup>b</sup>

<sup>a</sup>Department of Civil Engineering, MEF University, Istanbul, Turkey; <sup>b</sup>Department of Civil Engineering, Ozyegin University, Istanbul, Turkey

## ABSTRACT

The engineering purpose of a site-specific response analysis is to estimate the uniform hazard acceleration spectrum on the ground surface for a selected hazard level. One of the mandatory components for site response analyses is one or more representative acceleration time histories that need to be scaled with respect to the calculated seismic hazard level for the selected site. The selection and scaling procedures of earthquake acceleration records play an important role in this approach. The effects and differences in using two different scaling approaches are studied: scaling with respect to ground motion parameters and response spectrum scaling. A set of homogeneous ground motion prediction relationships are developed for peak ground acceleration, peak ground velocity, root-mean-square acceleration, Arias intensity, cumulative absolute velocity, maximum spectral acceleration, response spectrum intensity, and acceleration spectrum intensity based on a uniform set of acceleration records for ground motion parameter scaling.

The uncertainties associated with site response analysis are considered as epistemic and aleatory uncertainties in source characteristics, soil profile, and soil properties. Aleatory variability is due to the intrinsic randomness of natural systems; it cannot be reduced with additional data (Passeri et al. 2020), however; its variability may be modeled by probability distribution functions. Thus, one possibility is to determine the probability distribution of the acceleration spectrum calculated on the ground surface for all possible input acceleration records, site profiles, and dynamic soil properties. The variability in the earthquake source and path effects are considered using a large number of acceleration records compatible with the site-dependent earthquake hazard in terms of fault mechanism, magnitude, and distance range recorded on stiff site conditions. Likewise, a large number of soil profiles may be considered to account for the site condition variability. The uncertainties related to dynamic soil properties may be considered as possible variability of maximum dynamic shear modulus in site response analyses. A methodology is proposed to estimate a uniform hazard acceleration spectrum on the ground surface based on the probabilistic assessment of the factors involved in site response analysis. The uniform hazard acceleration spectra obtained from a case study are compared with the spectra calculated by probabilistic models proposed in the literature.

## ARTICLE HISTORY

Received 30 November 2020  
Accepted 5 October 2021

## KEYWORDS

site response; soil amplification; uniform hazard spectrum; strong ground motion

## 1. Introduction

A site-specific seismic hazard analysis is based on the regional seismic hazard assessment conducted to determine the uniform hazard acceleration spectrum (UHS) on the engineering bedrock outcrop. The ground motion characteristics on the ground surface vary significantly with respect to properties of soil and rock layers encountered in a soil profile. These differences would lead to variations in the amplitude, duration, and frequency content of acceleration time histories on the ground surface. An

important step in site-specific response analysis is the selection and scaling of the input acceleration records with respect to UHS on the rock outcrop. A relatively large number of acceleration records compatible with the site-dependent earthquake hazard in terms of fault mechanism, magnitude, and distance range recorded on stiff site conditions that became available during the recent decades may be used for site response analysis to account for the variability in the earthquake source and path factors. Since the effect of magnitude on the spectral accelerations is more significant than the effect of the epicentral distance, smaller tolerances may be considered for the magnitude and larger tolerances for the distance ranges (Rota, Lai, and Strobbia 2011). Besides, magnitude ranges need to be considered in the selection of the input acceleration time records with respect to different performance levels.

The variability of site conditions may be considered by conducting site response analyses for a large number of soil profiles. However, in most engineering projects, the number of available soil borings and observed soil profiles with all the geotechnical characterization may be limited. One option is to use Monte Carlo simulations for site parameters with respect to the layer thickness, shear wave velocity profiles, modulus degradations, and damping ratios (MRD).

The simplest option for selecting design ground motion acceleration spectra is to adopt contemporary ground motion prediction equations (GMPEs) formulated in terms of site and source classifications (Abrahamson, Silva, and Kamai 2014, Campbell and Bozorgnia, 2014; Boore et al. 2014). However, these formulations ignore all site-specific information and yield generic assessment of the design ground motion spectrum on the ground surface (Bazzurro and Cornell 2004a). Another option is to use empirical amplification factors suggested by Borcherdt (1994) based on average shear wave velocity,  $V_{s30}$ . The recorded ground motion data (Ansal, Tönük, and Kurtuluş 2015) and parametric studies (Baturay and Stewart 2003; Haase et al. 2011) indicate that the use of  $V_{s30}$  would yield unrealistic spectral accelerations on the ground surface, especially in the case of relatively soft or loose to medium soil layers and deep soil deposits. In addition, these deterministic procedures would yield surface ground motion levels with non-uniform, non-conservative, and inconsistent exceedance rates across the frequency range (Bazzurro and Cornell 2004b). In addition, Tsai (2000) observed that the hazard curve may be severely distorted if the soil nonlinearity is treated inadequately, and calculated results would likely overestimate the seismic hazard. The ground motion characteristics obtained empirically and linear amplification factors applied to bedrock motions are not enough to model nonlinear soil response. Due to uncertainties in estimating site amplification, the use of the median site amplification factors and the resulting ground motion is a hybrid answer that is not fully probabilistic (Aristizabal et al. 2018).

Lee and Anderson (2000) evaluated the residuals between the observed and GMPE calculated accelerations to establish correlations with respect to specific site parameters; however, it was not possible to establish reliable relationships, while Toro and Silva (2001) have proposed another approach by constructing a site-specific ground motion attenuation relation for each period of interest using a source-path-site random vibration theory (RVT) model that includes site amplification.

Site-specific probabilistic ground motion estimates may be based on site amplification distribution instead of a single deterministic median value. A probabilistic methodology using site amplification distributions to modify rock outcrop ground motion is considered (Cramer 2003). The use of a completely probabilistic approach can make about a 10% difference in ground motion estimates over simply multiplying a bedrock probabilistic ground motion by a median site-amplification factor with even larger differences at smaller probabilities of exceedance.

## 2. Site Response Methodology

### 2.1. Modified SHAKE

The proposed methodology is based on Equivalent Linear Site Response analyses accounting for soil nonlinearity conducted by the slightly modified version of Shake91 (Idriss and Sun 1992). The code was revised to include up to 8914 data points in input acceleration records and 50 modulus reduction

and damping ratio curves and 50 soil layers to account for the stress dependence (Darendelli, 2001). To account for frequency dependence (Yoshida et al. 2002), the relationship proposed by Sugito, Goda, and Masuda (1994) is adopted,

$$\gamma_{eff}(\omega) = C\gamma_{max}F(\omega)/F_{max}, \quad (1)$$

where  $C$  is a constant,  $\gamma_{max}$  is the maximum shear strain,  $F(\omega)$  is the Fourier spectrum of shear strain, and  $F_{max}$  represents the maximum of  $F(\omega)$  that is implemented into the code. The definition of  $\gamma_{eff}(\omega)$  on the left side of Eq. (1) is the equivalent strain, which controls equivalent shear modulus and damping ratio and is given proportional to the spectral amplitude of shear strain in the frequency domain. The limitations of the code pointed out by Lasley, Green, and Rodriguez-Marek (2014) are also accounted for to obtain more reliable results.

The effectiveness of frequency correction and stress-dependent modulus reduction and damping, as shown in Fig. 1, have improved the observed site response modeling using the recorded acceleration time histories in Ataköy strong motion station during  $M_w = 7.4$  Kocaeli 1999 Earthquake.

## 2.2. Reliability of Equivalent Linear Methodology

The advantages and limitations of equivalent linear site response analyses have been demonstrated by many researchers (Bolisetti et al. 2014; Chang et al. 1990; Stewart et al. 2008; Kramer and Paulsen 2004; Kim and Hashash 2013; Kaklamanos et al. 2013). The main purpose in this study, based on the applicability and reliability of the one-dimensional equivalent linear site response analysis, is to estimate the uniform hazard spectra (UHS) on the ground surface.

However, considering the suitability of vertical strong motion arrays, an attempt was made to test the applicability of the modified Shake code by modeling the earthquake records registered in relatively low-magnitude and distant earthquakes by the Istanbul Geotechnical Vertical arrays (Kurtuluş 2011).

In doing this modeling, to account for the possible variability of the measured shear wave velocity profiles, it is tried to modify the layer shear wave velocities by Monte Carlo simulations adopting normal distribution with various amounts of standard deviations. The fits obtained by minimizing the difference between recorded and calculated spectral accelerations by varying the shear wave velocity profile are not perfect as shown in Fig. 2. However, this may be considered acceptable from the engineering perspective. A similar approach by Kurtuluş (2011) yielded better fits for the same earthquakes and recorded accelerations.

## 3. Selection of Input Acceleration Records

Bommer and Acevedo (2004) and Bommer, Scott, and Sarma (2000) suggested to use real acceleration records for engineering analyses. The selection and scaling of input acceleration time histories is one of

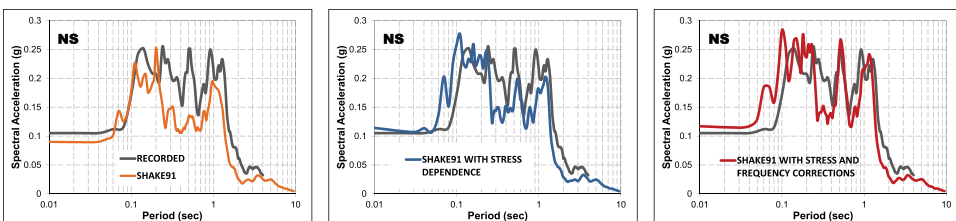
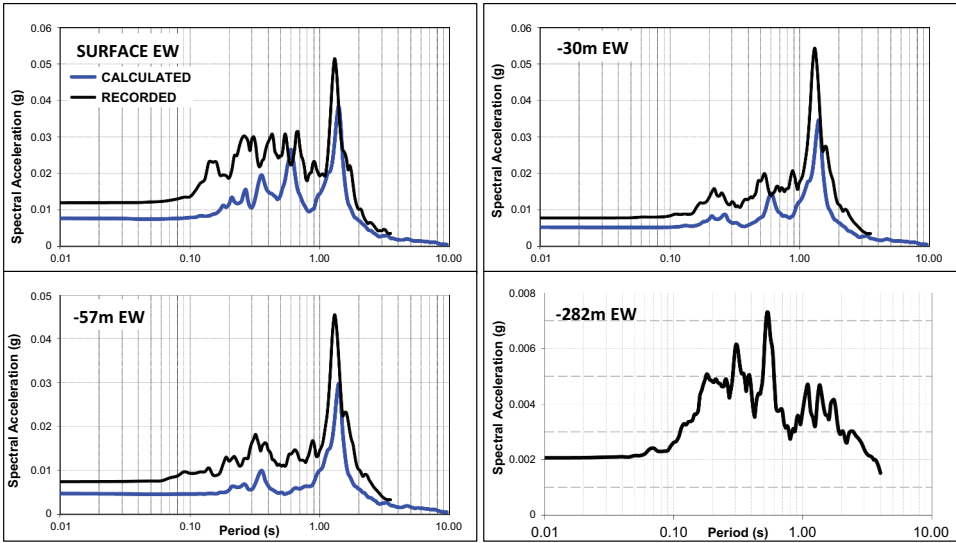


Figure 1. The effect of stress and frequency corrections for SHAKE91 modeling based on the recorded acceleration spectra at Ataköy SMS during 1999 Kocaeli Earthquake.



**Figure 2.** Recorded and calculated spectral accelerations at three depths and at the bedrock level in the Zeytinburnu vertical array for the 24.05.2014 Aegean Sea Earthquake of  $M_s = 6.5$ .

the major factors for site response analyses (Ansal et al. 2012; Haase et al. 2011; Tönük et al. 2013; Tönük and Ansal 2010). Kottke and Rathje (2011) and Rathje, Kottke, and Trent (2010) as well as the PEER Database (2019) developed procedures for selection and scaling of the suitable acceleration records.

The basic approach in selecting the input time histories is to select acceleration time histories recorded under similar tectonic systems for different spectral acceleration periods and exceedance probabilities. The approach adopted in site-specific investigations is to utilize the findings from the hazard analysis to select the probable fault type, magnitude, and distance ranges in the selection of the suite of acceleration time histories. Recorded time histories are selected from PEER Database (2019) on stiff site conditions with an average shear wave velocity of  $V_{s30} \geq 760$  m/s and within the range of  $\pm 10\%$  of expected  $M_w$  and  $\pm 30\%$  of the estimated fault distance based on hazard deaggregation (Bazzurro and Cornell, 1999). However, in some cases, in the selection of input acceleration records, it may be necessary to lower the average shear wave velocity threshold to  $V_{s30} \geq 500$  m/s for the recording station to be able to have a larger number of acceleration records. The findings from a preliminary parametric study conducted using 22 acceleration records from strong motion stations with  $V_{s30}$  are less than 500 m/s, and 22 different acceleration records from strong motion stations with  $V_{s30}$  larger than 500 m/s (Fig. 3a) indicate that the effect of the  $V_{s30}$  of the recording station may be negligible based on the acceleration spectra obtained on the ground surface from site response analysis on 209 different soil profiles from Zeytinburnu district in Istanbul (Ansal et al. 2010); thus, the range of  $V_{s30}$  values may be extended to increase the number of acceleration records. The difference between acceleration spectra with lower and higher  $V_{s30}$  may be compared with respect to the ratio of absolute differences divided by the spectral accelerations for stations with  $V_{s30}$  larger than 500 m/s as given in Fig. 3a. The mean difference ratio calculated to be 8.3% may be considered negligible considering the possible variabilities in the site response analysis.

One of the factors in the selection of the input acceleration time histories is the compatibility with respect to the fault type. A preliminary parametric study conducted for a site with 209 soil profiles, as shown in Fig. 3b, showed differences between the calculated response acceleration spectrum on the ground surface for the case of acceleration time histories

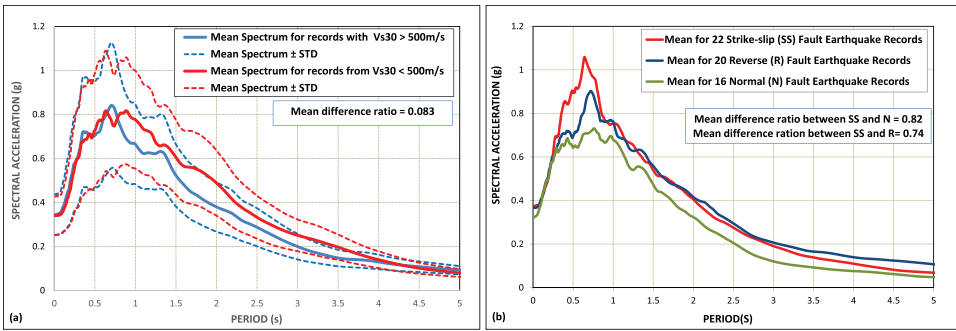


**Figure 3.** (a) The effect of  $V_{s30}$  of the recording station. (b) Effect of the fault type on the calculated acceleration spectrum on the ground surface.

recorded from strike slip, reverse, and normal faults. Thus, in the selection of hazard compatible records, compatibility with respect to possible fault types, earthquake magnitude, and source distance are important and they need to be considered in the selection procedure.

#### 4. Scaling of Input Acceleration Records

The scaling procedure becomes important to match the target peak ground acceleration and uniform hazard acceleration spectrum for different performance levels on the engineering bedrock outcrop. The adopted scaling procedure needs to have two major goals: (a) to obtain the best fits with respect to the target uniform hazard acceleration spectrum and (b) to decrease the scatter in the acceleration spectra after scaling.

##### 4.1. Scaling with respect to Ground Motion Parameters

The widespread option is to scale selected input acceleration records with respect to peak ground acceleration (PGA) from the probabilistic earthquake hazard analysis performed based on the available GMP relationships. However, other ground motion prediction equations would be needed to conduct scaling with respect to other ground motion parameters such as peak ground velocity (PGV), root-mean-square acceleration ( $a_{rms}$ ), Arias intensity ( $I_a$ ), cumulative absolute velocity (CAV), maximum spectral acceleration ( $SA_{max}$ ), response spectrum intensity (SI), and acceleration spectrum intensity (ASI).

The intended use of these engineering strong motion parameters primarily is to determine their effectiveness. Some of the parameters correlate well with several damage parameters of structural performance, liquefaction, seismic slope stability, vulnerability assessments, microzonation studies, etc. For example, for earthquake-resistant design, the earthquake ground motion defined is based on the elastic acceleration response spectrum. However, using the acceleration response spectrum in current seismic design practice does not directly account for the influence of the duration of strong motion or for the hysteretic behavior of the structure. Instead, a design approach based on input energy has the potential to address the effects of the duration and hysteretic behavior directly. Some examples for the use of engineering ground-motion parameters are generation of shake maps for rapid visualization of the extent of the expected damage to be used for emergency response, loss estimation, and public information (Wald et al. 1999); the development of early warning systems for the reduction of the seismic risk of vital facilities, such as nuclear power plants, pipelines, and high-speed trains; and estimation of damage potential due to liquefaction.

**Table 1.** Empirical attenuation coefficients and logarithmic standard deviation values for the geometric mean of the parameter calculated based on the mixed effects model.

$\ln(Y_{ij}) = b_1 + b_2M - b_3 * \ln(\sqrt{R_{JB}^2 + h^2}) + b_4 * \sqrt{R_{JB}^2 + h^2} + b_5F + \varepsilon_{ij}$							
Y	b1	b2	b3	b4	b5	h	$e_{ij}$
PGA	-1.3162	0.6086	1.5237	0.0040	0.0863	11.5547	0.537
RMSacc	-2.8283	0.6280	1.5653	0.0052	0.0829	10.9722	0.539
AI	-5.3938	1.6673	2.3296	0.0031	0.0295	10.1132	0.951
CAV	-6.1027	1.1047	0.7728	-0.0020	-0.0661	8.7406	0.461
SAmax	0.4803	0.5671	1.5016	0.0022	-0.0138	14.0440	0.560
ASI	-2.9416	0.7765	1.3941	0.0019	0.1138	11.8311	0.522
$\ln(Y_{ij}) = b_1 + b_2M - (b_3 + b_4M) * \ln(R_{JB} + 10) + b_5 * R_{JB} + b_6F_{ij}$							
Y	b1	b2	b3	b4	b5	b6	$e_{ij}$
PGV	6.8377	-0.0453	3.2451	-0.2950	0.0021	0.1115	0.648
SI	5.3856	0.2965	2.7515	-0.2343	0.0015	0.1831	0.710

The strong motion records used (given in Appendix Table A1) in this study are obtained from the NGA database maintained at the Pacific Earthquake Engineering Research Center (PEER) website because of its high quality and availability for the supplied information required and homogeneity due to the same processing procedures used. Proposed relations are derived using a subset (Table 1) of NGA data comprising 547 pairs of horizontal records obtained during 72 shallow crustal earthquakes with magnitudes  $4.5 < M < 7.9$  and hypocentral distances in the range of  $1 \text{ km} < r_{\text{hypo}} < 325 \text{ km}$  for the sites with average shear wave velocity at the upper 30 m,  $V_{s30} \geq 500 \text{ m/s}$ .

Only free-field records were used excluding records obtained in the basements of buildings, records in the first floor of buildings with three stories or higher, records at the dam toes, crests, and abutments in order to minimize the possible bias associated with the effects of such buildings in the recorded ground motion.

The records obtained from any earthquake with missing information such as stations without two horizontal components and stations without  $V_{s30}$  definition or earthquakes without fault mechanism information were also excluded from the analysis.

The predicted GMP relationships for eight engineering ground motion parameters (Table 1) for three magnitude bins ( $M = 4.5\text{--}5.5$ ,  $M = 5.5\text{--}6.5$ , and  $M = 6.5\text{--}7.5$ ) are plotted with respect to the calculated values from records in Fig. 4 for comparison purposes.

In order to evaluate the effect of the soil profile depth on scaling analysis, three soil profiles with similar equivalent shear wave velocities ( $V_{s30} = 267 \text{ m/s}$ ,  $294 \text{ m/s}$ ,  $304 \text{ m/s}$ ) but with different thicknesses were selected to conduct the parametric study (Tönük 2009).

All the results from the parametric site response study given in Table 2 with respect to the calculated peak ground acceleration (PGA) on the ground surface for three soil profiles with input time histories scaled with respect to eight scaling parameters are shown in Fig. 5 for the variation of the PGA standard deviation normalized with respect to the mean for the purpose of better comparison. The comparison results were not very different for PGV or  $SA_{\text{max}}$ .

The general parametric study on scaling with eight different scaling parameters on three damage parameters (PGA, PGV, and  $SA_{\text{max}}$ ) based on nine bins of magnitude and distance pairs for three soil profiles reveals that (1) when there are a large number of input motions, the variation of average damage parameter is not sensitive to the selected magnitude distance bin; (2) the soil profile depth is a dominating factor in the results, as the profile gets deeper, the selection of scaling parameters is not important; (3) the selection of scaling parameters is closely related to the damage parameter, the variance in the PGA and  $SA_{\text{max}}$  is smaller when the input motions are scaled with respect to acceleration-based parameters like PGA, Arias intensity, acceleration spectrum intensity, and the variance in the PGV is smaller when the input motions are scaled with respect to velocity-based parameters like PGV and cumulative absolute velocity; (4) SD/mean is a preferable comparison parameter, for which the minimum value may indicate the best scaling parameter.

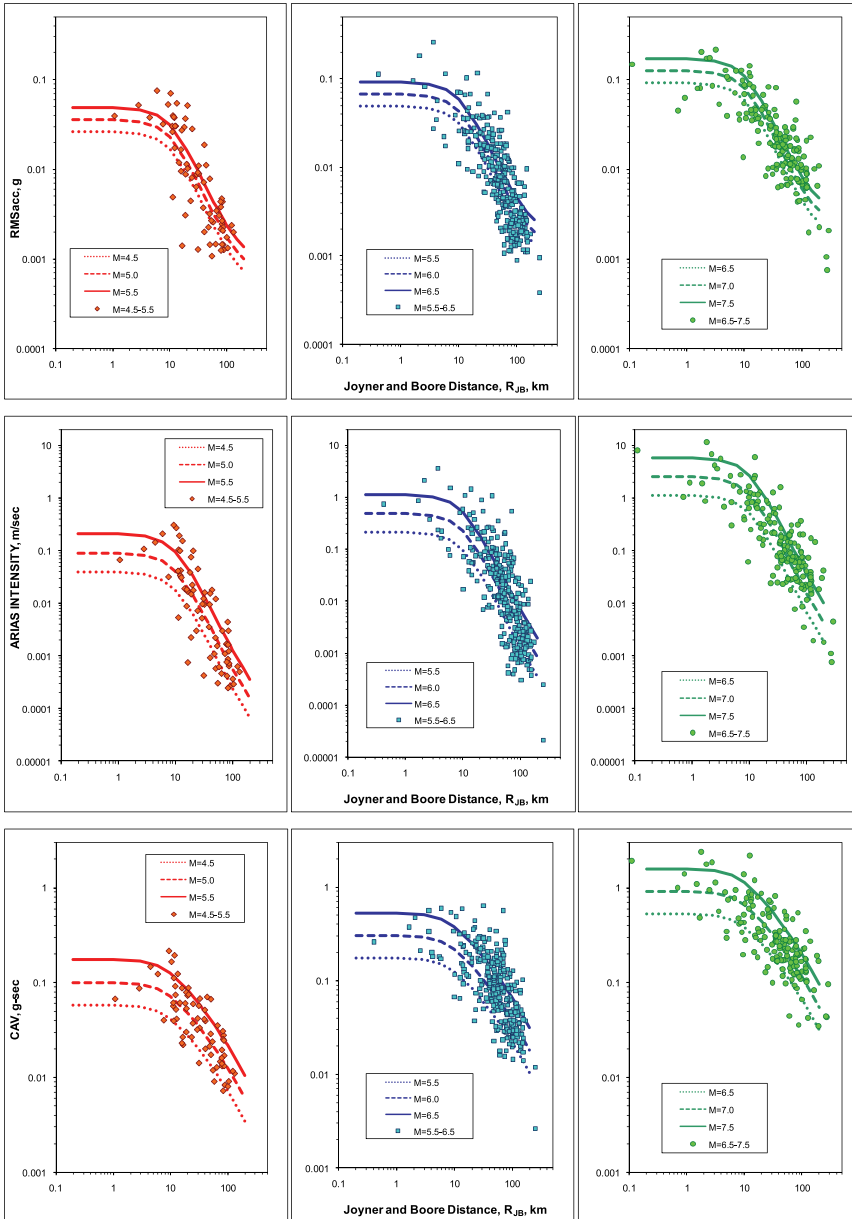


Figure 4. Selected ground motion parameters with observed data for bins of magnitude ranges.

The general outcome from this parametric study indicated that there are no significant distinctions among the selected eight strong motion parameters to be a more appropriate scaling parameter. Thus, another approach was developed to scale the selected hazard compatible input motions with respect to the uniform acceleration spectrum calculated on the rock outcrop.



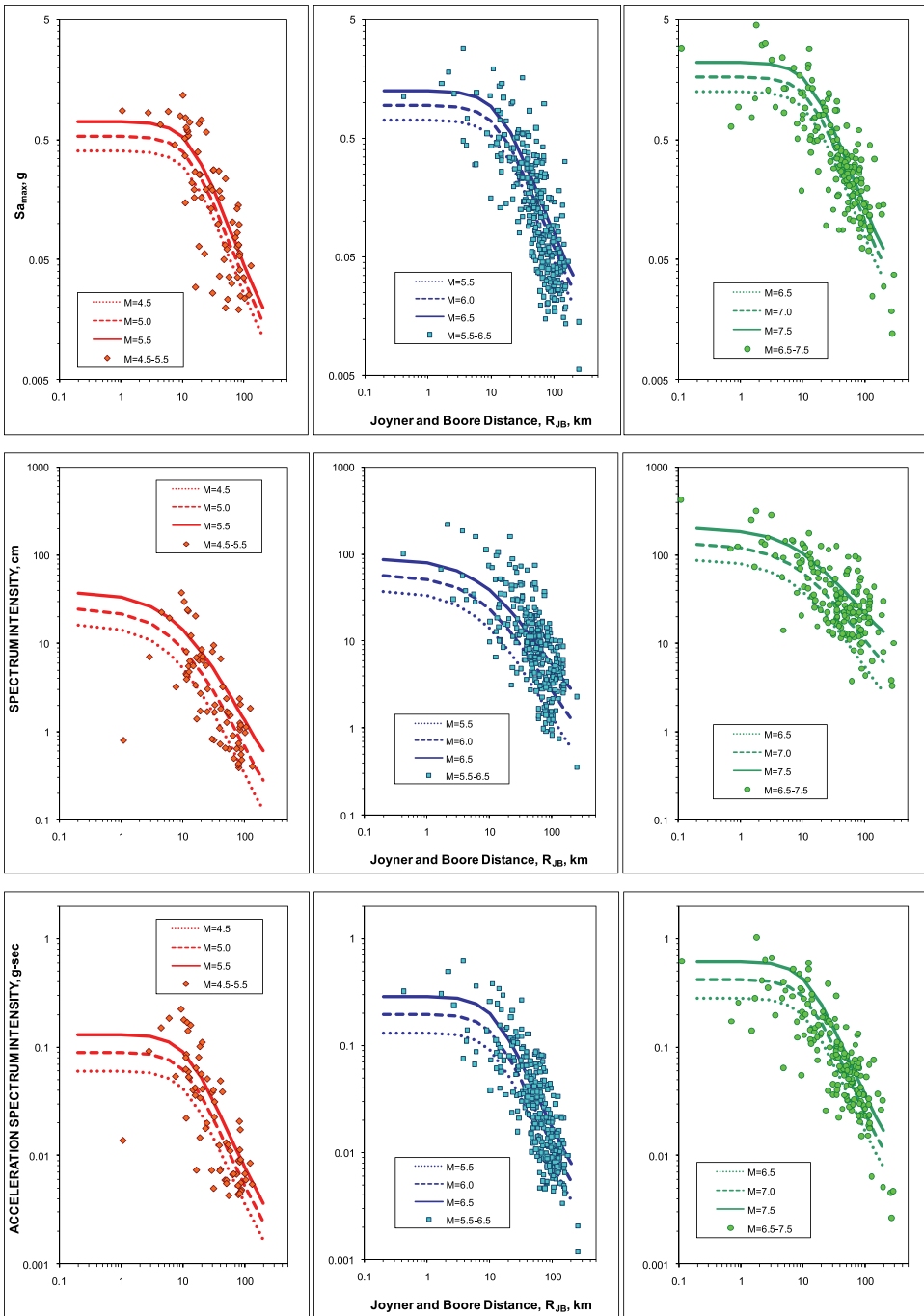
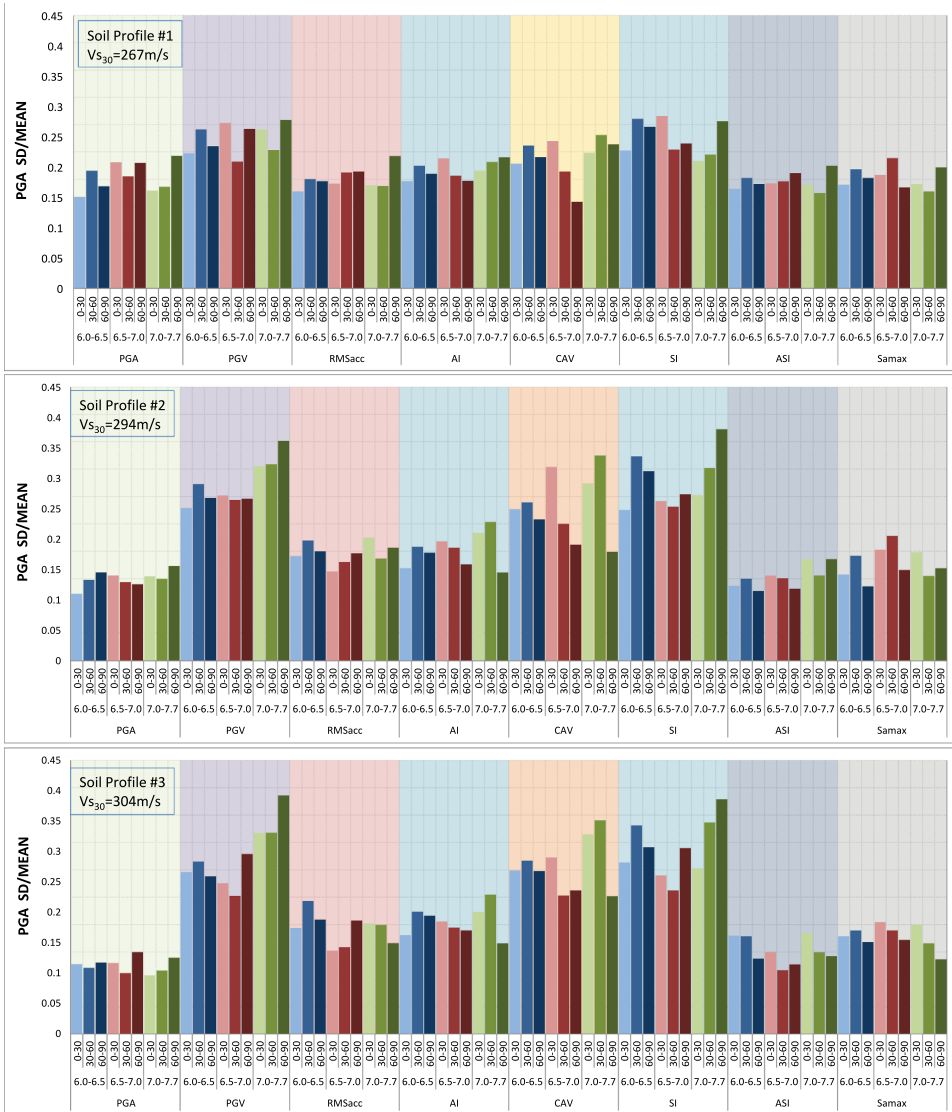


Figure 4. Continued.

**Table 2.** Magnitude and distance bins for the parametric scaling study.

Magnitude	Distance	No of input motions	Bin name
6.0– 6.5	0–30 km	45	1A
	30–60 km	92	1B
	60–90 km	64	1C
6.5– 7.0	0–30 km	34	2A
	30–60 km	31	2B
	60–90 km	26	2C
7.0– 7.7	0–30 km	49	3A
	30–60 km	49	3B
	60–90 km	31	3C



**Figure 5.** Variation of PGA SD/MEAN on the ground surface for the selected three soil profiles.

## 4.2. Spectrum Scaling

Spectrum scaling corresponds to scaling selected acceleration records individually to obtain the best fit for each with respect to the target acceleration spectrum by varying the peak acceleration without modifying the frequency content. This procedure is slightly modified from the mean spectra scaling (Ansal et al. 2012) that was based on the optimization of each record for the best fit of the mean spectrum with respect to the target spectrum.

Bazurro and Cornell (2004a, 2004b) reported that spectral acceleration is one of the effective ground motion parameters for the site amplification predictions. Therefore, the scaling of the selected records with respect to spectral acceleration would yield more consistent results. The scatter of the acceleration spectra for input acceleration records in terms of standard deviation is generally reduced in the case of the spectrum scaling approach (Ansal et al. 2018). It is important to decrease the scatter in the input level since it would also decrease the scatter during site response analyses and would lead to more consistent interpretation on the probabilistic evaluation of the UHS on the ground surface as shown in Fig. 6.

The other issue is the number of acceleration records to be used for site response analysis. A parametric study was conducted for a case study with 25 soil profiles, by varying the number of input acceleration records for site response analysis between 4 and 24. It was observed that the agreement between the mean acceleration spectra of the selected and scaled input acceleration records and target rock outcrop UHS is dependent on the number of selected acceleration records as shown in Fig. 7.

The observations indicate that in the range of 20–24 acceleration records, the ratio of the difference between the calculated mean spectrum and the target UHS on the rock outcrop is stabilized around 14% with only insignificant minor changes with additional input records. In the case of using a limited number of acceleration time histories, the mean spectra and standard deviation of all input records may be significantly different.

In addition, the number of acceleration records used for site response analysis would yield different mean acceleration spectra on the ground surface as shown in Fig. 7. The issue depends on the properties of the selected limited number of acceleration time histories, and the site response analyses would yield different results. The comparison of calculated mean acceleration spectra for 20 and 24 input acceleration records is very similar, indicating that for this case study, 20–24 acceleration inputs appear to be sufficient to calculate the mean spectral acceleration response spectrum on the ground surface.

## 5. Soil Profiles Used in Site Response Analysis

The other important source of variability in site response is the variability of the soil profile (Tran, Han, and Kim 2018). One option is to conduct as many site response analyses as possible, as in the approach adopted for the case of hazard compatible input earthquake acceleration records. The main question is to estimate the sufficient number of soil profiles to account for the variability of the site conditions. In large engineering projects, there can be a large number of borings.

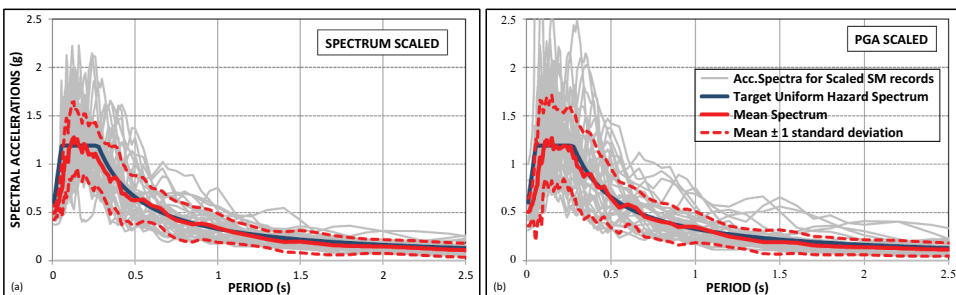


Figure 6. The difference of scatter between (a) spectrum and (b) PGA scaling for a single return period.

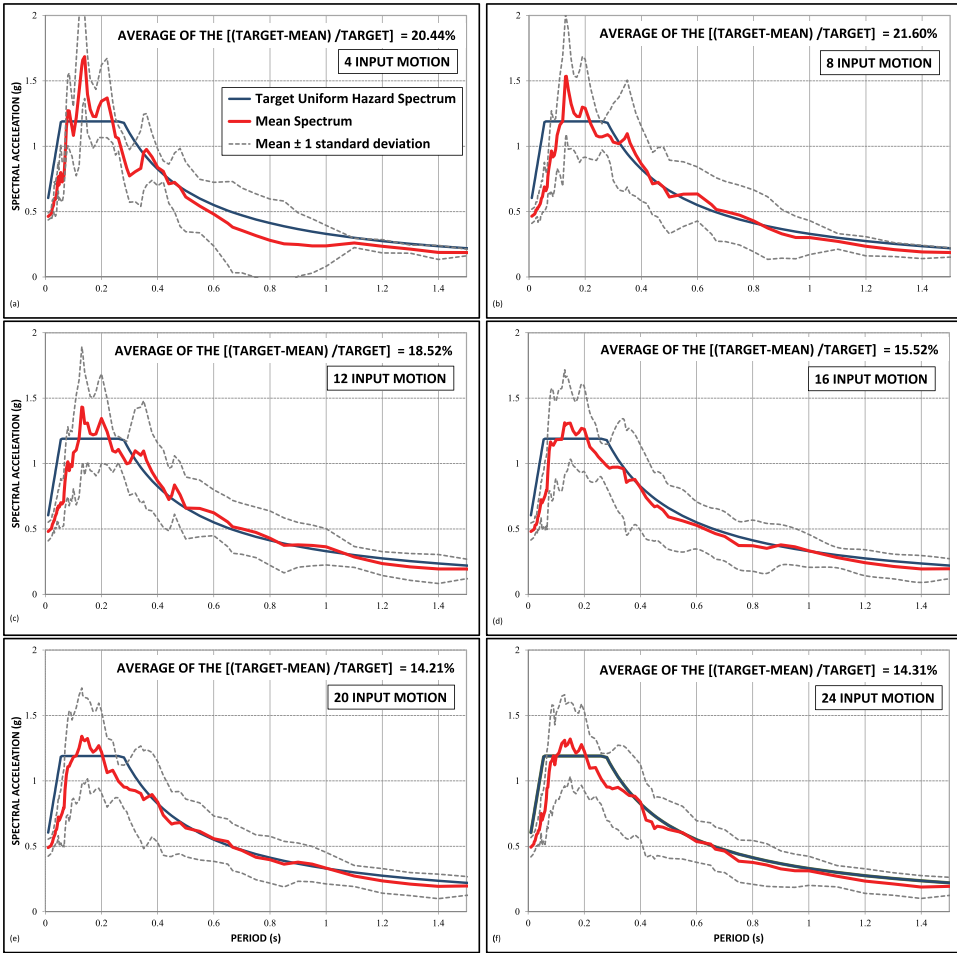
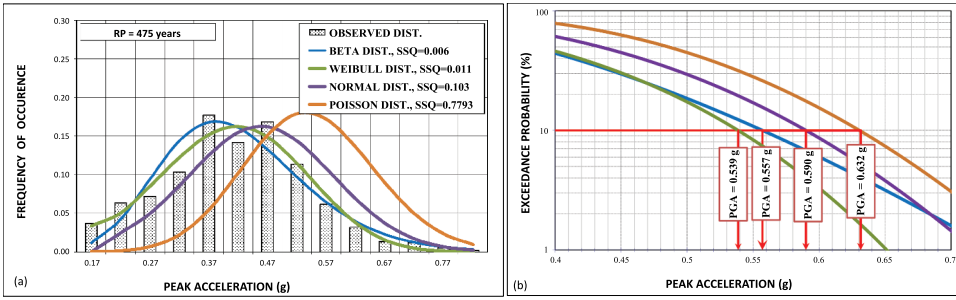


Figure 7. Effects of (a) 4, (b) 8, (c) 12, (d) 16, (e) 20, and (f) 24 input acceleration time histories on the ground surface.

Site response analysis was conducted for 25 existing shear wave velocity profiles using 24 input acceleration time histories (PEER 2019). It may be assumed that 600 site response analyses conducted may incorporate all the uncertainties in the basic factors (earthquake source and path, site conditions, and engineering properties of soil layers). Thus, probabilistic assessment of spectral accelerations on the ground surface may be based on the frequency distribution for each period to determine the best fitting distribution model.

Beta, Weibull, Gauss, and Poisson frequency distribution models are applied to the calculated peak ground accelerations on the ground surface as shown in Fig. 8. The Beta probability distribution model gave the best fit for the observed calculated PGA on the ground surface. Assuming that Beta distribution can model the scatter in the calculated PGA, thus, it would be possible to use the Beta probability function to estimate the PGA corresponding to 10% exceedance as  $\text{PGA} = 0.557 \text{ g}$ , while Weibull probability gave the lowest and Poisson probability gave the highest PGA, Fig. 8b. As shown in Fig. 8, Beta distribution is modeling frequency distribution better based on the SSQ (sum of the squares of the difference between observed and calculated). Based on this observation, in the second stage, the probability distribution of the calculated spectral accelerations is determined for each period level adopting Beta distribution as shown in Fig. 8.



**Figure 8.** (a) Comparison of various probability distribution models and (b) estimation of PGA corresponding to 10% exceedance probability on the ground surface.

The exceedance probabilities corresponding to 10% and 2% exceedance in 50 years are calculated using optimized fits with respect to Beta probability distribution for each period level based on 600 calculated acceleration response spectra. Thus, the probabilistic evaluation of the uniform hazard acceleration spectrum on the ground surface may be estimated.

The probabilistic modeling of frequency distribution by Beta distribution function, as can be observed in Fig. 9, may not model the observed distribution very accurately for all period levels. Thus, one other option, which requires less time, is to calculate based on a discrete approach, the 90% percentile value for each period level.

## 6. Probabilistic Evaluation of Site Response Analysis

An important factor controlling site response analyses is the site condition with respect to shear wave velocity and thickness assigned for each soil layer and thus the depth of engineering bedrock. The Monte Carlo simulation scheme has been adopted to study the effect of variability of the assigned shear wave velocities for each soil layer in a case study composed of 25 soil borings. The effect of variability is studied by generating Monte Carlo simulations (MCS) for 25 soil profiles assuming that the assigned shear wave velocities are mean values, and the range of possible variation is  $\pm 40\%$  of the mean. 100 soil profiles were generated for each 25 soil borings,

In the second case, again, a total of 60,000 site response analysis for 100 Monte Carlo simulations for 25 soil profiles for 24 acceleration records were conducted and the acceleration spectrum corresponding to 10% exceedance probability acceleration spectra is calculated. In the comparison of the acceleration spectra obtained with and without Monte Carlo simulations the difference is negligible. Thus, the initial proposal to adopt probabilistic interpretation of the calculated spectral acceleration distribution is applicable for defining the uniform hazard acceleration spectra on the ground surface and also for the case of the possible variability that may exist with respect to soil stratification.

The purpose is to define the uniform hazard spectrum on the ground surface, since Monte Carlo simulations were conducted on 25 soil profiles using 24 input motions with the total 60,000 runs, it is possible that the variability due to source and site conditions were taken into consideration, and thus, the UHS calculated on the ground surface may be acceptable as shown in Fig. 10 accounting for site and source variability.

### 6.1. Comparison with STRATA

At the last stage, it may be worthwhile to compare the UHS obtained on the ground surface with the proposed approach with the UHS obtained by some other approaches. The program STRATA (Kottke and Rathje 2008) was utilized to compare the results obtained with both procedures. In the STRATA

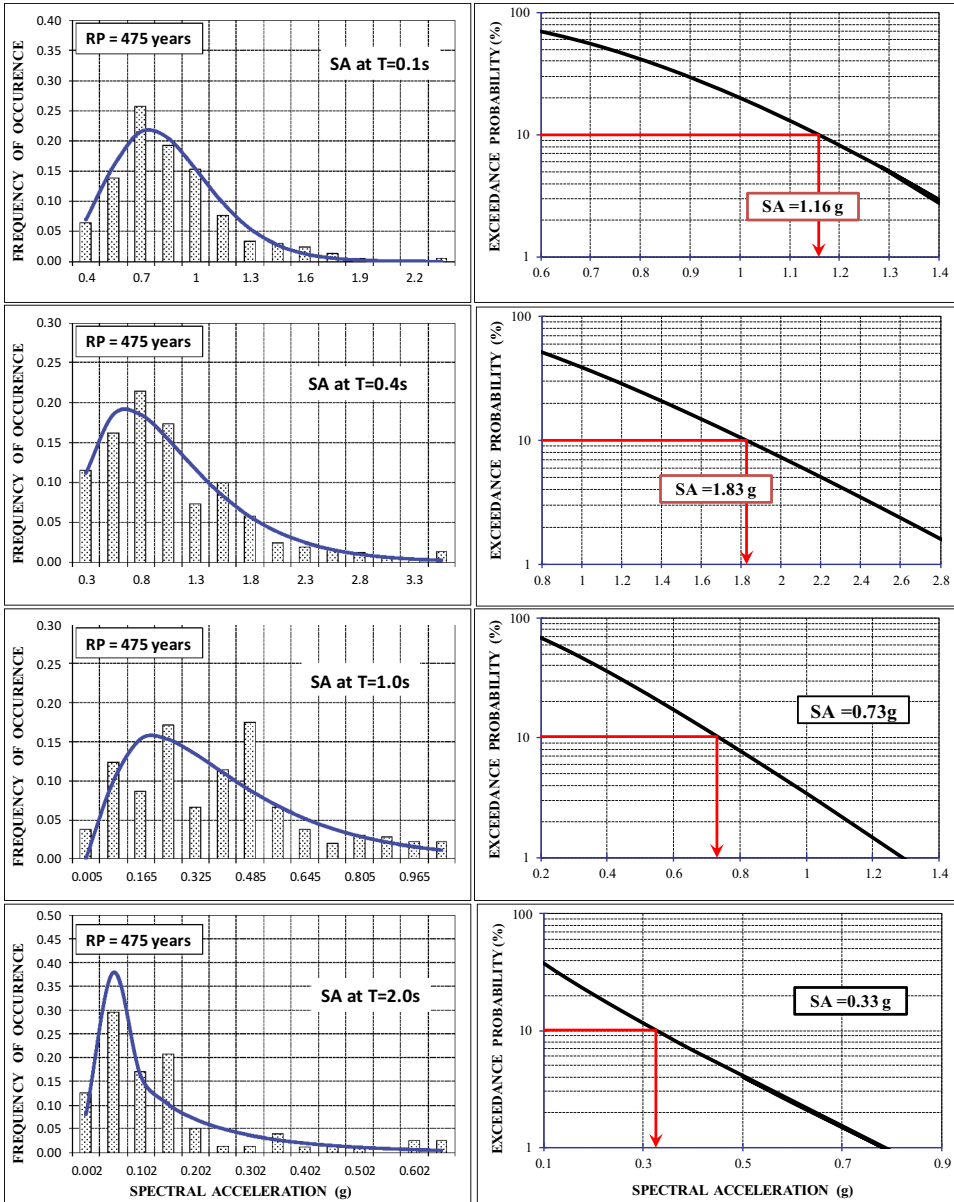


**Figure 9.** Comparison of Beta probability distribution models compared to discrete solution for spectral accelerations at different period levels.

As shown in Figs. 10, the 90% percentile spectrum for the 475year return period and the 98% percentile spectrum for 2475 year return period are very similar and slightly above the probabilistic spectra calculated by adopting the Beta distribution function.

code, there are two options: 1. UHS on the ground surface can be determined for any soil profile adopting random vibration theory (RV) and 2. the program also allows us to take into account variabilities in the layer thickness, shear wave velocity, modulus degradation, and damping. As shown in Fig. 11, for two real soil profiles, mean RV spectra for 100 simulations are similar to mean spectra for 2400 simulations by SHAKE91M and 10% exceedance spectra are similar to the 10% spectra calculated by the STRATA code using the random vibration approach.

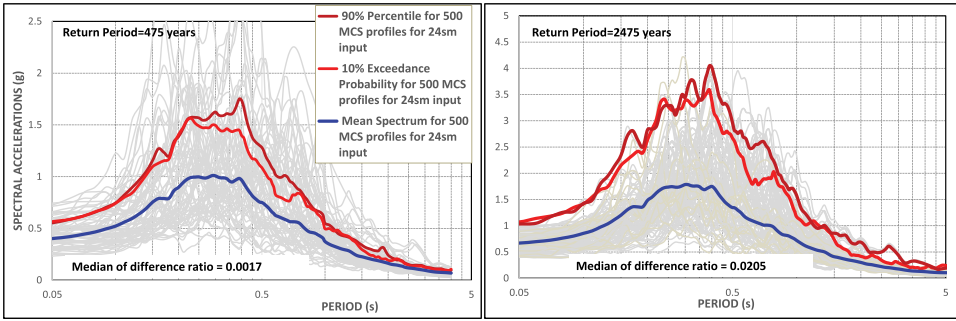


**Figure 10.** Mean acceleration spectrum with the uniform hazard spectrum calculated based on Beta distribution and discrete solution for RP = 475 and 2475 years for all and MCS generated soil profiles.

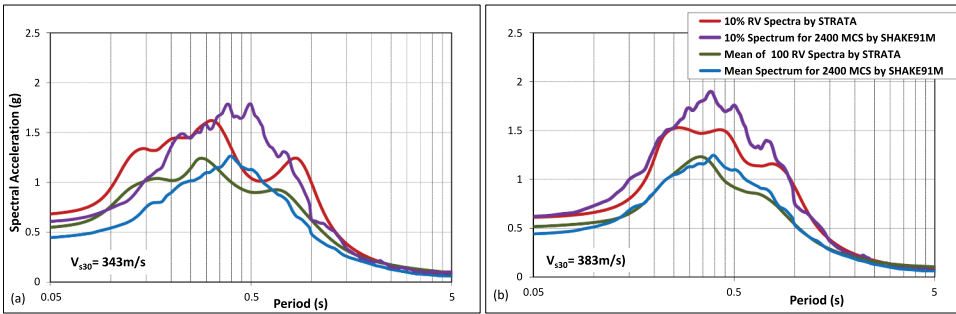


**Figure 11.** Comparison of the UHS for two different soil profiles (a) and (b) calculated based on SHAKE91M and STRATA.

## 7. Conclusions

An attempt was made to evaluate the probabilistic characteristics of an approach that may be adopted to develop uniform hazard acceleration design spectra on the ground surface corresponding to two performance levels of 475 and 2475 years return periods or to 10% and 2% exceedance probabilities in 50 years. A case study composed of 25 soil profiles obtained by site investigations was utilized in the parametric study. The proposed approach is based on performing a multiple number of site response analyses using 24 selected and properly scaled hazard compatible acceleration records. The design peak ground acceleration and uniform hazard acceleration spectra calculated based on these limited numbers of soil profiles are compared with respect to the site response results obtained from a large number of simulated soil profiles using the Monte Carlo simulation technique with respect to shear wave velocity and layer thickness encountered in the soil profiles. The results calculated for 475 year return period corresponding to 10% exceedance are not affected by the introduced variability with respect to layer shear wave velocity and layer thickness. Therefore, it appears possible to determine the design uniform hazard spectrum for 475 and 2475 years return periods based on Monte Carlo simulations accounting for the variability of source and site variabilities.

## Disclosure Statement

No potential conflict of interest was reported by the author(s).

## ORCID

A. Ansal  <http://orcid.org/0000-0003-1710-5557>

## References

- Abrahamson, N. A., W. J. Silva, and R. Kamai. 2014. Summary of the ASK14 ground motion relation for active crustal regions. *Earthquake Spectra* 30 (3): 1025–55. doi: [10.1193/070913EQS198M](https://doi.org/10.1193/070913EQS198M).
- Ansal, A., G. Tönük, and A. Kurtuluş. 2015. A probabilistic procedure for site specific design earthquake, Theme Lecture. 6th Int. Con. on Earthquake Geotechnical Engineering, Christchurch, New Zealand.
- Ansal, A., G. Tönük, and A. Kurtuluş. 2018. Implications of site specific response analysis. In *Recent Advances in Earthquake Engineering in Europe. ECEE 2018. Geotechnical, Geological and Earthquake Engineering*, ed. K. Pitilakis, 51–68. Springer.
- Ansal, A., G. Tönük, A. Kurtuluş, and B. Çetiner. 2012. Effect of spectra scaling on site specific design earthquake characteristics based on 1D site response analysis. Proc. of 15WCEE, Lisbon, Portugal.
- Ansal, A., G. Tönük, A. Kurtuluş, M. Erdik, and S. Parolia. 2010. Modeling the observed site response from istanbul strong motion network. Fifth International Conference on Recent Advances in Geotechnical Earthquake Engineering and Soil Dynamics, San Diego, CA -, May 24–29
- Aristizabal, C., P.-Y. Bard, C. Beauval, and J. Camilo Gómez. 2018. Integration of site effects into probabilistic seismic hazard assessment (PSHA): A comparison between two fully probabilistic methods on the euroseistest site. *Geosciences* 8 (8): 285. doi: [10.3390/geosciences8080285](https://doi.org/10.3390/geosciences8080285).
- Baturay, M., and P. Stewart. 2003. Uncertainty and bias in ground motion estimates from ground response analyses. *Bulletin of the Seismological Society of America* 93 (5): 2025–42. doi: [10.1785/0120020216](https://doi.org/10.1785/0120020216).
- Bazzurro, P., and C. A. Cornell. 1999. Disaggregation of seismic hazard. *Bulletin of the Seismological Society of America* 89 (2): 501–520.
- Bazzurro, P., and A. C. Cornell. 2004a. Nonlinear soil-site effects in probabilistic seismic-hazard analysis. *Bulletin of the Seismological Society of America* 94 (6): 2110–23. doi: [10.1785/0120030216](https://doi.org/10.1785/0120030216).
- Bazzurro, P., and A. C. Cornell. 2004b. Ground-motion amplification in nonlinear soil sites with uncertain properties. *Bulletin of the Seismological Society of America* 94 (6): 2090–109. doi: [10.1785/0120030215](https://doi.org/10.1785/0120030215).
- Bolisetti, C., A. S. Whittaker, H. B. Mason, I. Almufti, and M. Willford. 2014. Equivalent linear and nonlinear site response analysis for design and risk assessment of safety-related nuclear structures. *Nuclear Engineering and Design* 275: 107–21. doi: [10.1016/j.nucengdes.2014.04.033](https://doi.org/10.1016/j.nucengdes.2014.04.033).
- Bommer, J. J., and A. B. Acevedo. 2004. The use of real earthquake accelerograms as input to dynamic analysis. *Journal of Earthquake Engineering* 8 (sup001): 43–91. doi: [10.1080/13632460409350521](https://doi.org/10.1080/13632460409350521).
- Bommer, J. J., S. G. Scott, and S. K. Sarma. 2000. Hazard-consistent earthquake scenarios. *Soil Dynamics and Earthquake Engineering* 19 (4): 219–31. doi: [10.1016/S0267-7261\(00\)00012-9](https://doi.org/10.1016/S0267-7261(00)00012-9).
- Boore, D. M., J. P. Stewart, E. Seyhan, and G. A. Atkinson. 2014. NGA-West2 equations for predicting PGA, PGV, and 5% damped PSA for shallow crustal earthquakes. *Earthquake Spectra* 30 (3): 1057–85. doi: [10.1193/070113EQS184M](https://doi.org/10.1193/070113EQS184M).
- Borcherdt, R. D. 1994. Estimates of site dependent response spectra for design (methodology and justification). *Earthquake Spectra* 10 (4): 617–54. doi: [10.1193/1.1585791](https://doi.org/10.1193/1.1585791).
- Campbell, K. W., and Y. Bozorgnia. 2014. NGA-West2 ground motion model for the average horizontal components of PGA, PGV, and 5% damped linear acceleration response spectra. *Earthquake Spectra* 30: 1087–115.
- Chang, C. Y., C. M. Mok, M. S. Power, Y. K. Tang, H. T. Tang, and J. C. Stepp. 1990. Equivalent linear and nonlinear ground response analyses at Lotung seismic experiment site. Proceedings of the Fourth U.S. National Conference on Earthquake Engineering Earthquake Engineering Research Institute, Palm Springs, CA.
- Cramer, C. H. 2003. Site specific seismic hazard analysis that is completely probabilistic. *Bulletin of the Seismological Society of America* 93 (4): 1841–46. doi: [10.1785/0120020206](https://doi.org/10.1785/0120020206).
- Darendeli, M. B. 2001. Development of a new family of normalized modulus reduction and material damping curves. Ph. D. Dissertation, The University of Texas at Austin.
- Haase, J. S., Y. S. Choi, T. Bowling, and R. L. Nowack. 2011. Probabilistic seismic-hazard assessment including site effects. *Bulletin of the Seismological Society of America* 101 (3): 1039–54. doi: [10.1785/0120090322](https://doi.org/10.1785/0120090322).
- Idriss, I. M., and J. I. Sun. 1992. *Shake91, A computer program for conducting equivalent linear seismic response analysis of horizontally layered soil deposits*. Berkeley: University of California.
- Kaklamanos, J., B. A. Bradley, E. M. Thompson, and L. G. Baise. 2013. Critical parameters affecting bias and variability in site-response analyses using kik-net downhole array data. *Bulletin of the Seismological Society of America* 103 (3): 1733–49. doi: [10.1785/0120120166](https://doi.org/10.1785/0120120166).
- Kim, B., and Y. M. A. Hashash. 2013. Site response analysis using downhole array recordings during the March 2011 Tohoku-Oki earthquake and the effect of long-duration ground motions. *Earthquake Spectra* 29 (1\_suppl): 37–54. doi: [10.1193/1.4000114](https://doi.org/10.1193/1.4000114).



- Kottke, A. R., and E. M. Rathje (2008). *Technical manual for Strata*, Report No.: 2008/10. Pacific Earthquake Engineering Research Center, University of California, Berkeley.
- Kottke, A. R., and E. M. Rathje. 2011. A semi-automated procedure for selecting and scaling recorded earthquake motions for dynamic analysis. *Earthquake Spectra* 24 (4): 911–32. doi: [10.1193/1.2985772](https://doi.org/10.1193/1.2985772).
- Kramer, S. L., and S. B. Paulsen. 2004. Practical use of geotechnical site response models, Proceedings of the International Workshop on Uncertainties in Nonlinear Soil Properties and their Impact on Modeling Dynamic Soil Response, University of California, Berkeley, 10 pp.
- Kurtuluş, A. 2011. Istanbul geotechnical downhole array. *Bulletin of Earthquake Engineering* 9 (5): 1443–61. doi: [10.1007/s10518-011-9268-0](https://doi.org/10.1007/s10518-011-9268-0).
- Lasley, S. J., R. A. Green, and A. Rodriguez-Marek. 2014. Comparison Of equivalent-linear site response analysis software. Tenth U.S. National Conference on Earthquake Engineering, Anchorage, Alaska, July 21–25.
- Lee, Y., and J. G. Anderson. 2000. Potential for improving ground-motion relations in southern california by incorporating various site parameters. *Bulletin of the Seismological Society of America* 90 (6B): 170–S186. doi: [10.1785/0120000509](https://doi.org/10.1785/0120000509).
- Passeri, F., S. Foti, and A. Rodriguez-Marek. 2020. A new geostatistical model for shear wave velocity profiles. *Soil Dynamics and Earthquake Engineering* 136: 106247. doi: [10.1016/j.soildyn.2020.106247](https://doi.org/10.1016/j.soildyn.2020.106247).
- PEER. (2019). Pacific earthquake engineering research center, Strong Motion Database, <http://peer.berkeley.edu/>
- Rathje, E. M., A. R. Kottke, and W. L. Trent. 2010. Influence of input motion and site property variabilities on seismic site response analysis. *Journal of Geotechnical and Geoenvironmental Engineering* 136 (4): 607–19. doi: [10.1061/\(ASCE\)GT.1943-5606.0000255](https://doi.org/10.1061/(ASCE)GT.1943-5606.0000255).
- Rota, M., C. G. Lai, and C. L. Strobbia. 2011. Stochastic 1D site response analysis at a site in central Italy. *Soil Dynamics and Earthquake Engineering* 31 (4): 626–39. doi: [10.1016/j.soildyn.2010.11.009](https://doi.org/10.1016/j.soildyn.2010.11.009).
- Stewart J. P., A. O. Kwok, Y. M. A. Hashash, N. Matasovic, R. Pyke, Z. Wang, and Z. Yang. 2008. *Benchmarking of nonlinear geotechnical ground response analysis procedures*, PEER Report No. 2008/04, Pacific Earthquake Engineering Research Center, University of California, Berkeley, CA.
- Sugito, M., H. Goda, and T. Masuda. 1994. Frequency dependent equi-linearized technique for seismic response analysis of multi-layered ground. *Journal of Geotechnical Engineering, Proceedings of Of JSCE* 493: 49–58.
- Toro, G. R., and W. J. Silva. 2001. *Scenario earthquakes for Saint Louis, MO, Memphis, TN, and seismic hazard maps for the central United States region: Including the effect of site conditions*. Boulder, Colorado: Risk Engineering.
- Tönük, G. 2009. Factors affecting site response analysis. Ph.D.Thesis, Earthquake Engineering, Kandilli Observatory and Earthquake Research Institute, Boğaziçi University, Istanbul, Turkey
- Tönük, G., and A. Ansal A. 2010. Selection and scaling of ground motion records for site response analysis. 14th European Conference of Earthquake Engineering, Ohrid, paper no. 1386.
- Tönük, G., A. Ansal, A. Kurtuluş, and B. Çetiner. 2013. Site specific response analysis for performance based design earthquake characteristics. *Bulletin of Earthquake Engineering* 12 (3): 1091–105. doi: [10.1007/s10518-013-9529-1](https://doi.org/10.1007/s10518-013-9529-1).
- Tran, T., S. R. Han, and D. Kim. 2018. Effect of probabilistic variation in soil properties and profile of site response. *Soils and Foundations* 28 (6): 1339–49. doi: [10.1016/j.sandf.2018.07.006](https://doi.org/10.1016/j.sandf.2018.07.006).
- Tsai, C. C. P. 2000. Probabilistic seismic hazard analysis considering nonlinear site effect. *Bulletin of the Seismological Society of America* 90 (1): 66–72. doi: [10.1785/0119980187](https://doi.org/10.1785/0119980187).
- Wald, D. J., V. Quitoriano, T. H. Heaton, H. Kanamori, C. W. Scriver, and C. B. Worden. 1999. TriNet “ShakeMaps”: Rapid generation of peak ground motion and intensity maps for earthquakes in southern California. *Earthquake Spectra* 15 (3): 537–55.
- Yoshida, N., S. Kobayashi, I. Suetomi, and K. Muira. 2002. Equivalent linear method considering frequency dependent characteristics of stiffness and damping. *Soil Dynamics and Earthquake Engineering* 22 (3): 205–22. doi: [10.1016/S0267-7261\(02\)00011-8](https://doi.org/10.1016/S0267-7261(02)00011-8).

**Table A1.** Database of strong motion records used in the regression analysis.

No.	Earthquake Name	YEAR MODY HRMN	Hypocenter			Earthquake Magnitude	Mechanism Based on Rake Angle	Number of Stations
			Latitude (deg)	Longitude (deg)	Depth (km)			
1	San Francisco	1957 0322 1944	37.6700	-122.4800	8.0	5.28	Reverse	1
2	Parkfield	1966 0628 0426	35.9550	-120.4983	10.0	6.19	Strike Slip	1
3	Lytle Creek	1970 0912 1430	34.2698	-117.5400	8.0	5.33	Reverse Oblique	2
4	San Fernando	1971 0209 1400	34.4400	-118.4100	13.0	6.61	Reverse	6
5	Hollister-03	1974 1128 2301	36.9202	-121.4663	6.1	5.14	Strike Slip	1
6	Oroville-01	1975 0801 2020	39.4390	-121.5280	5.5	5.89	Normal	1
7	Oroville-03	1975 0808 0700	39.5020	-121.5120	7.6	4.70	Normal	1
8	Friuli, Italy-01	1976 0506 2000	46.3450	13.2400	5.1	6.50	Reverse	1
9	Friuli, Italy-02	1976 0915 0315	46.3750	13.0670	3.7	5.91	Reverse	1
10	Tabas, Iran	1978 0916	33.2150	57.3230	5.8	7.35	Reverse	2
11	Dursunbey, Turkey	1979 0718 1312	39.6600	28.6500	7.0	5.34	Normal	1
12	Coyote Lake	1979 0806 1705	37.0845	-121.5054	9.6	5.74	Strike Slip	2
13	Norcia, Italy	1979 0919 2136	42.7300	12.9600	6.0	5.90	Normal	2
14	Imperial Valley-06	1979 1015 2316	32.6435	-115.3088	10.0	6.53	Strike Slip	1
15	Livermore-01	1980 0124 1900	37.8550	-121.8160	12.0	5.80	Strike Slip	1
16	Livermore-02	1980 0127 0233	37.7370	-121.7400	14.5	5.42	Strike Slip	2
17	Anza (Horse Canyon)-01	1980 0225 1047	33.5050	-116.5140	13.6	5.19	Strike Slip	2
18	Victoria, Mexico	1980 0609 0328	32.1850	-115.0760	11.0	6.33	Strike Slip	1
19	Irpinia, Italy-01	1980 1123 1934	40.8059	15.3372	9.5	6.90	Normal	9
20	Irpinia, Italy-02	1980 1123 1935	40.8464	15.3316	7.0	6.20	Normal	7
21	Coalinga-01	1983 0502 2342	36.2330	-120.3100	4.6	6.36	Reverse	1
22	Coalinga-02	1983 0509 0249	36.2460	-120.2990	12.0	5.09	Reverse	1
23	Coalinga-03	1983 0611 0309	36.2560	-120.4500	2.4	5.38	Reverse	1
24	Coalinga-04	1983 0709 0740	36.2510	-120.4000	9.0	5.18	Reverse	1
25	Coalinga-05	1983 0722 0239	36.2410	-120.4090	7.4	5.77	Reverse	1
26	Coalinga-06	1983 0722 0343	36.2220	-120.4070	7.9	4.89	Reverse	1
27	Coalinga-07	1983 0725 2231	36.2290	-120.3980	8.4	5.21	Reverse	1
28	Coalinga-08	1983 0909 0916	36.2240	-120.2320	6.7	5.23	Strike Slip	1
29	Borah Peak, ID-02	1983 1029 2329	44.2390	-114.0700	10.0	5.10	Normal	2
30	Morgan Hill	1984 0424 2115	37.3060	-121.6950	8.5	6.19	Strike Slip	4
31	Lazio-Abruzzo, Italy	1984 0507 1750	41.7100	13.9020	14.0	5.80	Normal	1
32	Drama, Greece	1985 1109 2330	41.2253	23.9951	10.8	5.20	Normal Oblique	1
33	Nahanni, Canada	1985 1223	62.1870	-124.2430	8.0	6.76	Reverse	3
34	Hollister-04	1986 0126 1920	36.8040	-121.2847	8.7	5.45	Strike Slip	1
35	N. Palm Springs	1986 0708 0920	34.0000	-116.6117	11.0	6.06	Reverse Oblique	6
36	San Salvador	1986 1010 1749	13.6330	-89.2000	10.9	5.80	Strike Slip	1
37	Baja California	1987 0207 0345	32.3880	-115.3050	6.0	5.50	Strike Slip	1
38	Whittier Narrows-01	1987 1001 1442	34.0493	-118.0810	14.6	5.99	Reverse Oblique	10
39	Whittier Narrows-02	1987 1004 1059	34.0600	-118.1035	13.3	5.27	Reverse Oblique	2
40	Loma Prieta	1989 1018 0005	37.0407	-121.8829	17.5	6.93	Reverse Oblique	22
41	Roermond, Netherlands	1992 0413 0120	51.1700	5.9250	14.6	5.30	Normal	3
42	Cape Mendocino	1992 0425 1806	40.3338	-124.2294	9.6	7.01	Reverse	3
43	Landers	1992 0628 1158	34.2000	-116.4300	7.0	7.28	Strike Slip	3
44	Big Bear-01	1992 0628 1506	34.2100	-116.8300	13.0	6.46	Strike Slip	5
45	Northridge-01	1994 0117 1231	34.2057	-118.5539	17.5	6.69	Reverse	28
46	Kobe, Japan	1995 0116 2046	34.5948	135.0121	17.9	6.90	Strike Slip	4
47	Kozani, Greece-01	1995 0513 0847	40.1569	21.6746	12.6	6.40	Normal	2
48	Dinar, Turkey	1995 1001 1557	38.0600	30.1500	5.0	6.40	Normal	2
49	Kocaeli, Turkey	1999 0817	40.7270	29.9900	15.0	7.51	Strike Slip	7
50	Chi-Chi, Taiwan	1999 0920	23.8603	120.7995	6.8	7.62	Reverse Oblique	66
51	Duzce, Turkey	1999 1112	40.7746	31.1870	10.0	7.14	Strike Slip	5
52	Sitka, Alaska	1972 0730	56.7700	-135.7840	29.0	7.68	Strike Slip	1
53	Upland	1990 0228	34.1437	-117.6973	4.5	5.63	Strike Slip	1
54	Manjil, Iran	1990 0620	36.8101	49.3530	19.0	7.37	Strike Slip	1
55	Sierra Madre	1991 0628	34.2591	-118.0010	12.0	5.61	Reverse	2
56	Northridge-05	1994 0117 0043	34.3765	-118.6982	11.3	5.13	Reverse Oblique	2
57	Northridge-06	1994 0320 2120	34.2313	-118.4750	13.1	5.28	Reverse	13
58	Little Skull Mtn,NV	1992 0629	36.7200	-116.2860	12.0	5.65	Normal	3
59	Hector Mine	1999 1016	34.5740	-116.2910	5.0	7.13	Strike Slip	11
60	Yountville	2000 0903	38.3788	-122.4127	10.1	5.00	Strike Slip	3
61	Big Bear-02	2001 0210	34.2895	-116.9458	9.1	4.53	Strike Slip	2

(Continued)

**Table A1.** (Continued).

No.	Earthquake Name	YEAR MODY HRMN	Hypocenter		Depth (km)	Earthquake Magnitude	Mechanism Based on Rake Angle	Number of Stations
			Latitude (deg)	Longitude (deg)				
62	Anza-02	2001 1031	33.5083	-116.5143	15.2	4.92	Normal Oblique	13
63	Gilroy	2002 0514	36.9667	-121.5987	10.1	4.90	Strike Slip	7
64	Nenana Mountain, Alaska	2002 1023	63.5144	-148.1100	4.2	6.70	Strike Slip	3
65	Denali, Alaska	2002 1103	63.5375	-147.4440	4.9	7.90	Strike Slip	3
66	Big Bear City	2003 0222	34.3100	-116.8480	6.3	4.92	Strike Slip	5
67	Chi-Chi, Taiwan-02	1999 0920 1757	23.9400	121.0100	8.0	5.90	Reverse	58
68	Chi-Chi, Taiwan-03	1999 0920 1803	23.8100	120.8500	8.0	6.20	Reverse	46
69	Chi-Chi, Taiwan-04	1999 0920 2146	23.6000	120.8200	18.0	6.20	Strike Slip	38
70	Chi-Chi, Taiwan-05	1999 0922 0014	23.8100	121.0800	10.0	6.20	Reverse	52
71	Chi-Chi, Taiwan-06	1999 0925 2352	23.8700	121.0100	16.0	6.30	Reverse	47
72	Northridge-01	1994 0117 1231	34.2057	-118.5539	17.5	6.69	Reverse	1